CP505, *Shock Compression of Condensed Matter – 1999*
edited by M. D. Furnish, L. C. Chhabildas, and R. S. Hixson

PENETRATION DEPTH TIME HISTORY MEASUREMENT METHOD

C. Liu[1] and T. J. Ahrens[2]

[1] *Present address: Southwest Institute of Fluid Physics, Chengdu, PRC.* [2] *Seismological Laboratory 252-21, California Institute of Technology, Pasadena 91125 USA*

Abstract. A new method for measuring the depth time history of rigid body penetration into brittle materials under a deceleration of $\sim 10^5$ g. The method includes: sabot-projectile, sabot-projectile separation and penetration depth detection systems. Relatively small intrinsic time error (3%) and depth error (0.3-0.7 mm) results. Penetration depth time history in a series of 4140 steel projectile penetrations into a mortar are measured at velocities of 100 to 500 m/sec with sufficient accuracy such that differentiation with respect to time yields stopping force, via Newton's second law.

INTRODUCTION

Penetration time history measurements provide crucial information of penetration dynamics. The measurement methods employed in previous works include high-speed photography (1), laser Doppler anemometry (2), and on-board accelerometers (3). The understanding of rigid penetration into various soft materials (soils) has been improved using on-board instrument measurements (3 and 4). However, for high-strength brittle materials such as hard rocks, low temperature ice and various concretes, a knowledge of rigid penetration dynamics is still deficient because of lack of proper methods to measure penetration time history due to very high decelerations. Measured deceleration is applied in Newton's second law to determine stopping force. We report the method we developed to measure the depth time history of rigid penetration into brittle materials.

MEASUREMENT METHOD

The basic principle of the present method is to measure the time history of the projectile position, relative to any stationary point in the target. Thus the projectile penetration depth-time history in the target is obtained. The projectile body is assumed to be rigid during penetration.

The present method includes three crucial elements: (1) Projectile and sabot; (2) Sabot-projectile separator; (3) Detection system. Figure 1 gives the experimental arrangement inside the Caltech 40 mm gun tank.

Projectile and sabot design: Because a projectile body is basically used as a ruler to measure depth, black and white stripes are put on the projectile lateral surface as labels. In order for the label method to work accurately, two issues considered are the stripe width and integrity during launch. Stripe widths are important because they affect both temporal and spatial measurement accuracy. However, there are some limitations imposed by machining and the detection system. Based on the relationship between stripe width and reflected laser energy (5) and the limitations, the actual widths used in experiments are 0.3 and 0.7 mm for white and black stripes, respectively.

Previous methods used to launch projectiles with a large length-to-diameter ratio (6 and 7) damage stripes during launch and sabot-projectile separation. In order to launch projectiles without any damage to stripes, the projectiles are designed to be held by a combination sabot that consists of aluminum and plastic sabots as shown in Figure 1. Most importantly, upon machining the projectile-sabot assembly, it is crucial to ensure that the projectile axis aligns with the sabot axis to prevent failure during launch or sabot stripping.

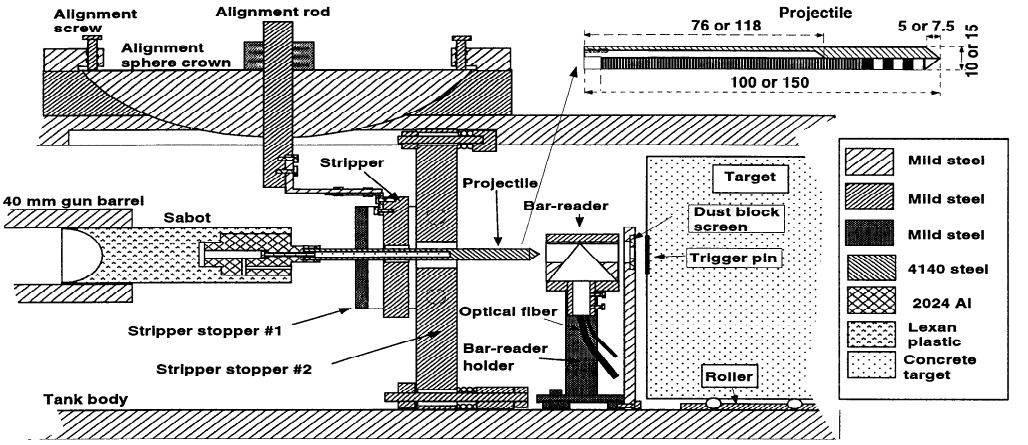

Figure 1: Experiment set-up. Stripper and bar-reader are aligned with axis of 40 mm gun barrel using a laser beam. Stripper stopper #1 is used to protect barrel from impact of stripper that may bounce back after it strikes stripper stopper #2 (SS#2). SS#2 is designed to prevent stripper and sabots from following projectile. Also SS#2 prevents propellant products from interfering with bar-reader during measurement. Target (0.5 m diameter and 0.4 - 0.6 m long) sits on a roller and is fixed to the tank body after it is aligned with the gun. Insert shows projectile affixed with black/white stripe pattern in present study. All dimensions are in mm.

Projectile and sabot separation: In order to conduct penetration measurements free of interference from the sabot, it is necessary to separate the sabots from the projectile immediately after they exit the gun barrel. The key issue in the design of the sabot-projectile separation system is to ensure that the separation process does not disturb the projectile trajectory and has a minimal effect on projectile velocity. This appears to be more important for low velocities (10^2 m/s). The sabot-projectile separation system used in this work is shown in Figure 1. Because the projectile velocity is relatively low, separation takes a relatively long time, which means that asymmetries in the stripper assembly must be properly considered. Otherwise reflected waves from the stripper edges may influence the projectile trajectory. The two criteria used to design the stripper are: (1) sabots should not plug the stripper plate after the sabots impact the stripper, (2) the diameter must be large enough so that waves reflected back from the plate edge do not interfere with separation process, i.e., that asymmetries on the plate edges will not affect projectile trajectory. Based on these two criteria, the stripper plate dimensions were designed to be 20 mm in thickness and 140/200 mm in diameter for initial impact velocity was higher/lower than 200 m/s when the stripper material is 4120 steel.

Detection system: In order to detect all stripes passing over a laser beam with high enough time and spatial resolution, the detection system must collect reflected laser energy very efficiently. Three major factors that affect laser energy collection are (1) laser energy reflected from the surface is not spatially uniform, (2) the direction of maximum reflected laser energy may vary with time during penetration due to possible misalignment , (3) dust particles from impact and burned propellant products may obscure the laser beams. Based on the above conditions, the designed system (Figure 2) includes (1) a VISAR probe (FOP-1000, Valyn International) was chosen to focus and also collect laser energy. (2) laser trap #1 and #2 are used to reflect part of the laser energy from misaligned and/or non-diffusive surfaces back to the probe, and (3) original 1 mm diameter plastic fiber is replaced with 2 mm diameter plastic fiber

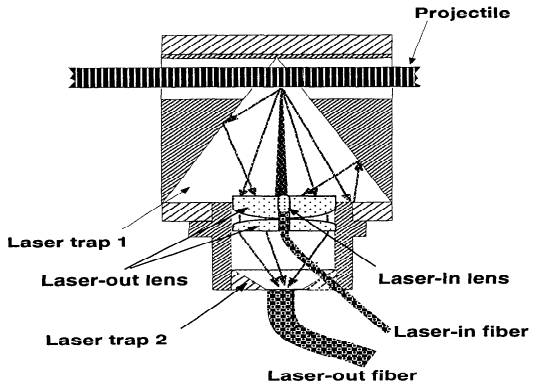

Figure 2: Schematic of bar-reader cross-section.

(DuPont) to increase laser collection efficiency. During penetration, the projectile velocity varies from the initial impact velocity (10^2 m/s) to very low velocity (10 m/s). This large velocity change requires the recording system to have a bandwidth of 10 kHz to 20 MHz. Two different kinds of photodiodes with built-in amplifiers are chosen. One (C5331-11, Hamamatsu) has the bandwidth from 10 kHz to 80 MHz and the other (C30833, RCA) from 4 kHz to 5 MHz.

Error analysis: The intrinsic time error comes from stripe width uncertainty and the rigid body assumption. The boundary between black and white stripes does not necessarily have a sharp and straight edge due to machining imperfections, but instead it could be diffuse and wavy. This results in timing error of

$$\delta t_1 = \frac{L_{wb}}{v}, \tag{1}$$

where L_{wb} is average boundary width and v is projectile velocity.

Elastic waves generated from the initial impact reverberate in the projectile body. This wave reverberation changes the effective stripe width due to strain associated with elastic waves. The maximum width change of one pair of black and white stripes induced by the elastic wave is therefore $\delta L = (L_w + L_b)u_e^a/C_e$ in which u_e^a and C_e are particle and longitudinal elastic wave velocity in projectile material, respectively. The time error, δt_2, related to the width change is

$$\delta t_2 = \frac{\delta L}{v} = \frac{(L_w + L_b)}{v}\frac{u_e^a}{C_e}. \tag{2}$$

Therefore, the possible maximum time error during the penetration process is given by a summation of Eqs. (1) and (2) as $\delta t = \delta t_1 + \delta t_2$. Then, the percentage intrinsic time error, Er, is

$$Er = \frac{100\delta t}{(L_b + L_w)/v} = 100(\pm\frac{u_e^a}{C_e} \pm \frac{L_{wb}}{L_w + L_b}). \tag{3}$$

For the experiments conducted, the typical values of $L_w + L_b$, L_{wb} and v are 1 mm, 0.01 mm and 200 m/s, respectively. C_e is 5.3 km/s for 4140 steel. Elastic wave amplitude is taken to be approximately 50% of the peak pressure just after impact, $\sigma_e^a = 0.4$ GPa since the measurement point is far away from the impact site (~20 mm). From Eq. (3), the maximum error is estimated to be $\sim$ 3 %.

Although a trigger pin is used to give the exact time at which a projectile starts to penetrate into a target, the projectile position is not determined precisely because of the finite stripe width (the same thing is true for penetration stop point).

Therefore, the maximum uncertainty of the position at which a projectile starts to penetrate and stops penetrating

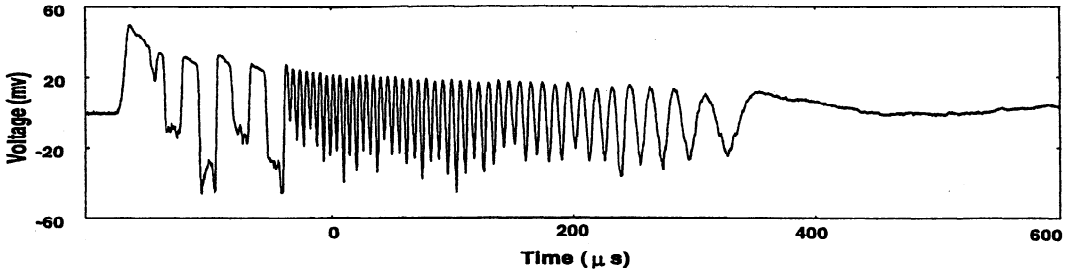

Figure 3: Typical experimental record of reflected laser amplitude Shot 1033. Detection of wide stripes at 180 to -130 μsec is indicated.

is half of the stripe width. The width is either black or white stripe width depending on where the laser beam hits at that particular moment. Therefore, the maximum uncertainty of the penetration start and stop point ranges from 0.15 to 0.35 mm.

METHOD VALIDATION

Using the designed systems and 40 mm gas/powder gun at Caltech, a series of 4140 steel projectile penetration into G-mixture mortar experiments was conducted. Typical reflected laser amplitude recorded is shown in Figure 3. The penetration depth and deduced penetration velocity time histories are shown in Figure 4. Experimental results demonstrate that the systems operated successfully. The validity of the experimental results is demonstrated by:

(1) Final penetration depth: Table 1 compares the final penetration depth determined by the penetration depth-time measurement with that measured from the recovered targets. The two depths are in good agreement, clearly demonstrating that the present method yields a complete penetration depth time history.

(2) Initial projectile velocity: The initial projectile velocity was also determined using laser obstruction. Because projectiles passed through the bar-reader before they started to penetrate into targets, the initial impact velocity after projectile-sabot separation was also measured by the present method. The good agreement between the two measured velocities (Table 1) shows that the separation system does not affect projectile velocity.

CONCLUSIONS

A penetration depth time history measuremental method was developed. For the first time, a whole penetration depth-time history was recorded with a very dense datum point under 10^5 g deceleration. The results provide dynamic constrains to theoretical models and numerical simulations.

ACKNOWLEDGMENTS

This work was supported by NASA and AFOSR. Contribution number 8662, Division of Geological and Planetary Sciences, California Institute of Technology.

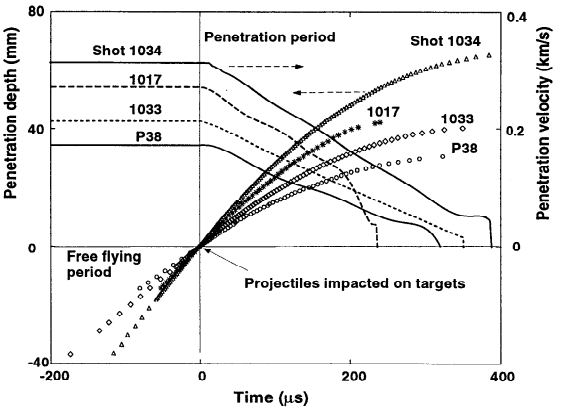

Figure 4: Penetration depth and velocity versus time. Solid and dashed lines are deduced penetration velocity.

Table 1: Experimental parameters.

Shot	Depth[1]	Depth[2]	V[1] (m/s)	V[2] (m/s)
P38	30.2±0.5	30.4±0.3	172.2±1.0	178.0 ±0.1
1017	41.4±1	42.2±0.3	265.7± 2.3	272.5 ± 0.3
1033	40.5±0.6	40.3±0.7	215.4 ± 0.7	213.3 ± 0.5
1034	66.7±1	65.2±0.7	320.5 ± 2.1	321.4 ± 3.0

Depth$^{(1)}$ (cm) and Depth$^{(2)}$ (cm) are penetration depth measured in recovered targets and by this method, respectively. V$^{(1)}$ and V$^{(2)}$ are projectile velocity obtained from laser obstruction methods and this method.

References

[1] Zhu G., W. Goldsmith and C. K. H. Dharan, *Int. J. Solids Structures* **29**, 399-420, (1992).

[2] Wu E., H. Sheen, Y. Chen and L. Chang, *Experimental Mechanics* **34**, 93-99, (1994).

[3] Forrestal, M. J. and V. K. Luk, *Int. J. Impact Engng.*, **12**, 427-444, (1992).

[4] Backman, M. E. and W. Goldsmith, *Int. J. Engng. Sci.*, **16**, 1-99, (1978).

[5] Liu, C., Brittle material response to shock loading, PhD Thesis, California Institute of Technology, 1999.

[6] Anderson, W. W., T. J. Ahrens, A. Gibson, R. Scott, and K. Suzuki, *J. Geophys. Res.* **101**, 21,137-21,149, (1996).

[7] Stilp, A. J. and V. Hohler, Experimental methods for terminal ballistics and impact physics in *High Velocity Impact Dynamics*, edited by J. A. Zukas, published by John Wiley& Sons, Inc., New York, 1990, 515-592.